

# DEBLURRING OF IMAGES USING BLIND SCHEMES

A THESIS SUBMITTED IN PARTIAL FULFILLMENT OF THE  
REQUIREMENTS FOR THE DEGREE OF

Master of Technology  
in  
Computer Science and Engineering

By

Pushpanjali Sahu



DEPARTMENT OF COMPUTER SCIENCE AND ENGINEERING  
NATIONAL INSTITUTE OF TECHNOLOGY  
ROURKELA

2007

# DEBLURRING OF IMAGES USING BLIND SCHEMES

A THESIS SUBMITTED IN PARTIAL FULFILLMENT OF THE  
REQUIREMENTS FOR THE DEGREE OF

Master of Technology  
in  
Computer Science and Engineering

By

Pushpanjali Sahu

Under the Guidance of

Prof. B. Majhi



DEPARTMENT OF COMPUTER SCIENCE AND ENGINEERING  
NATIONAL INSTITUTE OF TECHNOLOGY  
ROURKELA

2007



**National Institute of Technology  
Rourkela**

**CERTIFICATE**

This is to certify that the thesis entitled, "**Deblurring of Images Using Blind Schemes**" submitted by Ms. **Pushpanjali Sahu** in partial fulfillment of the requirements for the award of Master of Technology in "Computer Science & Engineering " at the National Institute of Technology, Rourkela (Deemed University) is an authentic work carried out by her under my supervision and guidance.

To the best of my knowledge, the matter embodied in the thesis has not been submitted to any other University / Institute for the award of any Degree or Diploma.

Place : NIT Rourkela  
Date :

**Dr. B. MAJHI**  
Professor  
Dept. of Computer Science & Engg.  
National Institute of Technology  
Rourkela - 769008.

## ACKNOWLEDGEMENT

*A blend of gratitude, pleasure and great satisfaction is what I feel to convey my indebtedness to all those who directly or indirectly contributed to the successful completion of this Thesis. I express my profound and sincere gratitude to my Guide, Prof. B.Majhi, Prof., CSE, whose Persistence guidance and support helped me in the successful completion of the work in stipulated time. His expert knowledge and scholarly suggestion help me to visualize the difficulty aspects of the thesis and to find their design solution.*

I am grateful to Dr. S. K. Jena, Head of the Department, Computer Science and Engineering, NIT Rourkela for his support during my work. My sincere thanks goes to Pankaj Kumar Sa, Lecturer, Computer Science and Engineering for his constant motivation. I am thankful to all my Professors and Lecturers and members of the department for their generous help in various ways for the completion of the thesis work.

I am thankful to all my batchmates and friends for their effective cooperation. Thank you Tony, Anamika, Mita, Kalpana, Madhu.

Lastly, but not the least, I am deeply indebted to my parents and my brothers for their constant support, encouragement and understanding during the voyage. I can offer here only an inadequate acknowledgement of my appreciation to my *family*.

Pushpanjali Sahu

# Contents

<b>List of Figures</b>	<b>vi</b>
<b>List of Tables</b>	<b>vii</b>
<b>1 INTRODUCTION</b>	<b>1</b>
1.1 Formulating Image Restoration Problem . . . . .	3
1.2 Problem Statement . . . . .	4
1.3 Key Motivation for Blind Image Deconvolution . . . . .	5
1.4 Problem Characteristics . . . . .	6
1.5 Blind Image Deconvolution Techniques at a Glance . . . . .	7
1.6 Thesis Overview . . . . .	10
<b>2 INTRODUCTION TO IMAGE BLUR</b>	<b>11</b>
2.1 The Point Spread Function,PSF . . . . .	12
2.1.1 Types of Blur . . . . .	12
2.2 Modeling space-invariant Blur . . . . .	14
2.3 Motion Blur . . . . .	15
2.4 Gaussian Blur . . . . .	17
2.5 Simulated Result . . . . .	17
<b>3 BLIND DECONVOLUTION USING EVOLUTIONARY ALGORITHM</b>	<b>19</b>
3.1 Applications of Evolutionary Algorithm, EA . . . . .	21
3.2 Multiobjective Optimization using EA . . . . .	22
3.3 EA for Blind Deconvolution . . . . .	22
3.4 Underlying Assumptions . . . . .	22
3.5 Underlying Constraint on PSF and Image . . . . .	24
3.6 Convergence Criteria . . . . .	24

3.7	Realizing BID using EA . . . . .	24
3.8	Image fusion using <i>pseudo-wigner distribution, PWD</i> . . . . .	26
3.9	Simulation Results of EA . . . . .	27
<b>4</b>	<b>TWO PASS HEURISTIC APPROACH FOR MOTION BLUR PARAMETER IDENTIFICATION</b>	<b>30</b>
4.1	Motivation for Blur Identification . . . . .	31
4.2	Theoretical Background . . . . .	32
4.3	Implementing the Algorithm . . . . .	34
4.4	Simulation Result . . . . .	37
<b>5</b>	<b>CONCLUSIONS AND FUTURE WORKS</b>	<b>41</b>
	<b>Bibliography</b>	<b>43</b>

# Abstract

The thesis presents two blind deconvolution schemes for image blur removal. The two major types of blur has been worked out, namely, the *gaussian blur* and the *motion blur*. The image corrupted by the *gaussian blur* is reconstructed by Evolutionary algorithm using *pseudo-wigner distribution*. The second method deals with heuristically estimating the blur parameter of the image undergone motion blur. The gaussian effect is mostly observed in astronomical imaging. The image deblurring for motion blurred image is required due to hardware incapability of capturing the exact information of moving object or with moving camera. In this thesis, an observed image is assumed to be the two dimensional convolution of the true image with a linear-shift invariant blur, known as *point-spread function, psf*, and the additive noise is assumed to be zero.

The Evolutionary algorithm has been implemented to remove gaussian blur. The atmospheric turbulence is mostly modelled by the *gaussian psf*. The algorithm proceeds by randomly generating the *psf's* at each generation. The *psf's* at each generation are used to estimate the true image. The best fitted images are then given as input to the next generation. After few generation, the most feasible images are chosen. These closer estimated images are fused using *pseudo-wigner distribution* to reconstruct the final required image.

The inherent dynamic characteristic of the nature gives rise to motion blur. Whenever there is relative motion between the object to be captured and the imaging system, the image captured at that instant is suffered by the type of blur known as *motion blur*. A new heuristic approach has been framed out with the purpose of estimating the *motion blur* parameter. This type of blur is characterised by its length and the motion direction. These parameters are then used to restore the image. The motion direction is estimated from the fourier domain of the observed motion blurred image. The length is then iteratively computed using *Entropy* and the *RMSE* as the quality metrics.

# List of Figures

1.1	Image Degradation and Restoration Process . . . . .	3
2.1	Image formation with PSF . . . . .	13
2.2	Result for different blur effect. . . . .	18
3.1	General scheme of EA . . . . .	21
3.2	General scheme of BID using EA . . . . .	26
3.3	Gaussian Blurred Lena Image and Restored Lena Image . . . . .	28
3.4	More Gaussian Blurred Image Lena Image and Restored Image . . . . .	28
3.5	Gaussian effected Lena Image . . . . .	29
3.6	Gaussian blurred lake image with varying value of standard deviation. . . . .	29
4.1	Motion Blurred Lena Image with varying angle and its corresponding Fourier Spectrum . . . . .	36
4.2	Plotted Entropy of images. . . . .	38
4.3	Entropy plot of images. . . . .	39
4.4	(a)Lena image blurred with psf length=11 and angle=23. (b) Restored image. . . . .	39



# List of Tables

3.1	Algorithm for PSF generation . . . . .	25
4.1	Algorithm . . . . .	37
4.2	Results of Observed Blur Parameter . . . . .	40

# **Chapter 1**

## **INTRODUCTION**

Vision is the foremost trusted source of information compare to other human perceptions. And *Image* is the basic container of any pictorial information . The process of retrieving and analyzing the pictorial information by a digital computer is known as *digital image processing*. The improvement of pictorial information for human interpretation and processing of scene data for autonomous machine perception are the root application areas that had sown the interest in image processing field decades ago[6].

Ideally, when an image is generated from a physical process, its values are proportional to energy radiated by a physical source. And hence, the resultant image,  $i(x,y)$ , is *nonzero* and *finite*[5], i.e.,

$$i(x, y) \in \mathcal{Z} \quad (1.1)$$

where  $\mathcal{Z}$  is a finite set of integers, and  $x, y$  denote spatial coordinates. Hence, an *image* is interpreted as a two-dimensional light intensity function,  $i(x, y)$ , and the value of  $i$ , at any point  $(x, y)$  is propotional to the brightness(or gray level) of the image at that point[5]. A digital image can be considered as a matrix whose row and column indices represent point in the image and the corresponding matrix element known as *picture element, pixels* value identifies the gray level at that point. The *digital image processing* takes as input an image always but the output can be an image or some relevant information retrieved after applying some function on the given input image. The various methods included as fundamental techniques of digital image processing are[5]:

1. Image Representation and Modeling
2. Image Enhancement
3. Image Restoration
4. Image Analysis
5. Image Reconstruction
6. Image Data Compression

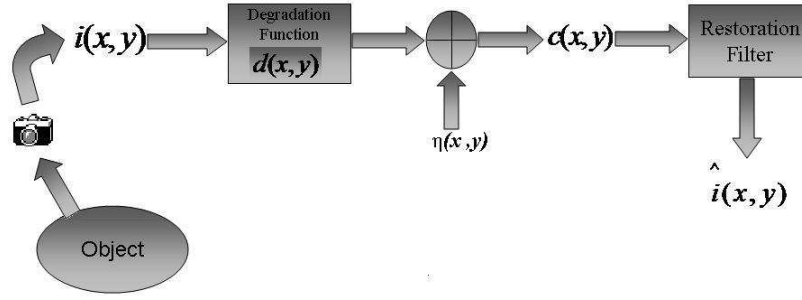


Figure 1.1: Image Degradation and Restoration Process

The image processing technique dealt in this thesis is *image restoration*. Image restoration has been explored a lot till date but much has to be mined of still. From the wide broad spectrum of image restoration, only a part is worked out in this thesis, reconstruction of the true image and blur parameter estimation.

## 1.1 Formulating Image Restoration Problem

The image is characterized by two major components : *illumination* and *reflectance* components. But, practically apart from these two components, the image formation also depends on the characteristics of the object being captured, environmental conditions during capture, and the imaging system being used. These other components produce an ill-effect during image acquisition to produce a degraded image,  $c$ . The process of reconstructing the original scene from a degraded version is the goal of *image restoration*. The ill-effect causing function,  $d_f$  is known as the *blur*. The additive noise effect is also considered as another cause of degradation. Thus, the image degradation model is,

$$c = d_f i + \eta \quad (1.2)$$

Given  $c$ , some knowledge about the degradation function  $d_f$ , and some knowledge about the additive noise term  $\eta$ , the objective of restoration is to obtain an estimate  $\hat{i}$  of the original image. This estimate,  $\hat{i}$ , should be as close as possible to the original input image. In general, the more knowledge we have about  $d_f$  and  $\eta$ , the closer  $\hat{i}$  will be to  $i$ . Figure 1.1 shows the image degradation and restoration process.

Image restoration refers to removal or minimization of known degradations in an

image. The process includes deblurring of images degraded by the limitations of a sensor or its environment, noise filtering, and correction of geometric distortion or non-linearities due to sensors.

The image restoration had found its break through application in the engineering community in the area of astronomical imaging. Due to rapidly changing index of refraction of the atmosphere, ground-based imaging systems were subject to blurring[3]. Extraterrestrial observations of the earth and the planets were degraded by motion blur as a result of slow camera shutter speeds relative to rapid space-craft motion. Till today, key focus area of image restoration is astronomical imaging. Another challenging area where image restoration play a very important part is in the area of medical imaging. The media also, particularly movies, even remain untouched by image restoration. The use of digital techniques to restore aging and deteriorated films is also important and well-known application area of image restoration. Digital image restoration is being used in many other applications as well, say, for example, lastly but not the least, to improve federal aviation inspection procedures, restoration has been used to restore blurry X-ray images of air craft wings[11].

## 1.2 Problem Statement

Image deconvolution refers to the act of discovering the original image from the observed corrupted image. The *blind image deconvolution*, *BID*, refers to the task of separating two convolved signals,  $i$  and  $d$ , when both the signals are either unknown or partially known[1]. The recovery process or reconstructing process can be subdivided into two categories as:

1. Classical Restoration
2. Blind Image Restoration

Classical restoration includes the techniques that utilize some prior information regarding the degradation of image during reconstruction while *Blind Image restoration* is the process of estimating both the true image and the blur from the degraded image characteristics, using partial information or no information about the imaging system. In classical restoration, the blurring function is given and the degradation process is inverted using one of the many known restoration algorithms. In blind

image deconvolution, an observed image  $c(x, y)$ , is assumed to be the two dimensional convolution of the true image  $i(x, y)$  with a linear-shift invariant blur, known as *point-spread function*,  $d(x, y)$  and the additive noise is assumed zero[1]. That is,

$$c(x, y) = i(x, y) * d(x, y) \quad (1.3)$$

The problem of reconstructing the true image  $i(x, y)$  requires the deconvolution of the  $PSF, d(x, y)$  from the degraded image,  $i(x, y)$ . A lot of research has been done exploring the various methods for image deconvolution as blind techniques. But still, is a critical and challenging problem for the researchers.

### 1.3 Key Motivation for Blind Image Deconvolution

Inspite of being difficult problem, the blind image deconvolution has enjoyed wide application area in most of the practical scenarios. The major motivations behind *blind image deconvolution* can be focused as:

1. Use of high cost adaptive-optics systems to overcome the blurring problem in astronomical imaging is impractical for analyzing some observation. Instead the blind deconvolution is cheapest way to retrieve the relevant information from the degraded image as a post-processing technique.
2. Some application area such as medical imaging rely on high image quality for close diagnosis, like X-ray imaging, which inturn demands for increased incident X-ray beams intensity. But practically, this is hazardous for patients health and hence blurring is inevitable. Hence, *BID* is used to tackle with the degradation.
3. Instant deblurring cannot be done by predetermining certain  $PSF$  in real-time applications such as video-conferencing. Also, on-line degradation determining technique is error prone and create artifacts in restored image.
4. Lastly, but not least, to predetermine any information about any scenario is practically either too costly, or dangerous and sometimes mostly impossible. Also, the degradation specified is not necessary true for deblurring. Hence, blind approach is adopted to solve the problem.

## 1.4 Problem Characteristics

The *blind deconvolution of image* proceeds based on certain assumptions. The problem of blind deconvolution of image has few characteristics as listed below:-

1. The convolved signals, i.e, the true image and the *psf* are irreducible[1]. This is the most important characteristic for the unambiguous deconvolution. The true image(or the *psf*) should not be resultant of convolution of two or more other independent different component signal. Let us assume that the true image,  $i(x, y) = i_1(x, y) * i_2(x, y)$  and the *psf*,  $d(x, y) = d_1(x, y) * d_2(x, y)$ , then the image model can be re-written as :-

$$c(x, y) = i_1(x, y) * i_2(x, y) * d_1(x, y) * d_2(x, y) \quad (1.4)$$

Hence, the deconvolution would be ambiguous as its quite difficult to clearly classify the true image component and the *psf* component.

2. The blind image deconvolution produces the scaled, shifted version of the true image. So,

$$\hat{i} = Ai(x - b_1, y - b_2) \quad (1.5)$$

where  $A, b_1, b_2$  are arbitrary real constants and  $\hat{i}$  is the estimation of original image. This shifted and scaled version is again treated using some other information as support constraint etc. to further improve the result[1]. But the blind deconvolution cannot find  $A, b_1, b_2$ .

3. Many of the blind deconvolution techniques assume noiseless condition for reconstruction. But, the noise persists in every practical scenerio. Hence, neglecting the noise while reconstruction obviously effect the result.
4. The blind deconvolution is ill-posed problem. The solution set may entirely change even with small variation in the assumed data sets used for reconstruction. Moreover, modelling the data set for exact deconvolution is not an easy task. Also, the exact deconvolution demands for consistent data set which is not applicable for every practical scenerio.
5. The imaging system may also be noisy. So, the noisy imaging system may also

lead to false result. The noise information is statistical in nature, so the direct subtraction is also not possible[1].

6. The resultant is obtained based on one or the other optimal criteria, which in turn rely on some partial information about the imaging procedure. The additional assumptions and proper initialization is required for proper result. Hence, the solution is not unique.
7. The three important factors namely convergence property, computational complexity and portability altogether are hard to meet in a single existing blind deconvolution technique. There exists no clear demarcation for all three mostly the convergence property. Also, the properties are not fixed but have to variate as the imaging system as well as imaging procedure and application varies. Let, say, for example, in real-time imaging application there is requirement of less computational complexity and speedy convergence while in medical imaging, the reliability plays an important role for good result as compare to other two.

## 1.5 Blind Image Deconvolution Techniques at a Glance

The process of separating two signals that have been convolved is termed as the *deconvolution* problem. When both the signals are unknown, it comes under the category of blind technique. The separation of signals using blind deconvolution technique proceeds with some distinguishing characteristics of both the signals that has to be deconvolved. Some signal characteristics must be known and those characteristics has to be kept as nonspecific as possible in order to achieve the solution. There are wide applications of blind deconvolution in seismic, speech, signal processing and ofcourse, in image processing.

The blind deconvolution in image processing first started in the area of astronomical imaging. Due to rapidly changing refractive index of the atmosphere, the ground-based imaging system suffered from blurring. This was first scenerio for applying restoration technique but the various practical applications demand for blind deconvolution still today. The blind deconvolution of images are done by following either of the two approaches[1] :-

1. The degradation function,  $psf$ , is identified and then using any classical restoration



technique such as inverse filtering, weiner filtering, pseudoinverse filtering, the true image is identified. This method is simple and less computation is required. The algorithms in this approach are known as a *priori blur* identification technique.

2. The identification of the *psf* and the *true image* is done simultaneously in the restoration algorithm. Hence the algorithms in this approach are complex.

Based on these two approaches, the various existing blind image deconvolution techniques is classified. Lane and Bates approach for multidimensional deconvolution is based on the concept that any degraded image,  $c$ , can be deconvolved if the individual convolved components,  $i_1, i_2, \dots, i_n$ , have compact support and  $c$  has dimension greater than one[14]. Their method exploit the analytical properties of Z-transform for deconvolving the degraded image. The technique is known as **zero sheet separation** . This method is based on assumptions such as :

- The imaging system is noiseless.
- The true image,  $i$ , and the degradation function,  $d$  are irreducible. The ZT of each  $i(x, y)$  and  $d(x, y)$  is zero on a single continuous surface, known as zero sheet[14].
- The zero sheets of  $i(x, y)$  and  $d(x, y)$  are distinct.
- The true image and the degradation function have finite support.

This method can also be utilized for deconvolving more than two signals. But this approach is prone to noise.

*A priori* blur identification techniques are the simplest blind deconvolution techniques. The degradation function is estimated first and the true image is estimated. The approach shows the promising results once the blurring parameters are estimated. The technique is applicable to the situations in which the true image is known to possess special features, and/or when the degradation function is known to be of special parameteric form. One of the most popular method of this category for blur identification is use of frequency domain nulls of the degraded image to perform blind deconvolution [15]. The algorithm is sensitive to noise, since the noise has the effect of masking the frequency domain nulls of observed image. The algorithm is improved by considering the noise effect by Tekalp [17] by using the bicepstrum instead of the cepstrum. Though the cepstrum method is more popular due to its computational

complexity. The major limitation of the algorithms of this class is that a parameteric form of the degradation function has to be known.

Another class of blind image deconvolution include nonparameteric deterministic image constraints restoration techniques. The algorithms of this group assume some deterministic constraints for estimating the true image. These deterministic constraints are like non-negativity, known finite support and existence of blur invariant edges. The methods apply these constraints as optimal criteria. The *true image* and the *blur* both are identified simultaneously. The two most popular methods of this group are:-

- Iterative Blind Deconvolution first proposed by Ayers and Dainty [18]. This is the simplest blind technique till date. The method uses the Fast-Fourier transform(FFT) for reconstructing the true image and the *psf*. The algorithm starts with some random initial guess about the true image,  $i(x, y)$ . With this initial estimate, the algorithm proceeds iteratively computing the *psf* and the true image. The technique utilizes some *a priori* information regarding  $i(x, y)$  and  $d(x, y)$ . The observed image can be noisy or can be noiseless. The algorithm alternates between the image domain and the fourier domain. The fourier domain constraint is imposed while dealing with fourier components and similarly, the image domain constraint is enforced while estimating the image and the blur. The algorithm is preferred for its low computational complexity[1]. The entire computation is done in the fourier domain which is cheaper and faster than the spatial domain operation. But the major drawback is that the algorithm is unstable. The algorithm is modified for robustness against noise by using weiner-filter instead of inverse filter by Deepa Kundur [1]. The solution uniqueness and convergence criteria are not fixed.
- Nonnegativity and Support Constraints Recursive Inverse Filtering(NAS-RIF) was proposed as a solution to problems associated with the poor convergence properties of the iterative blind deconvolution [1]. The method involves the iterative minimization of a convex cost function. The image is restored by filtering the blurred image to produce an image estimate which is restricted to lie on a convex set representing the known deterministic constraints of the true image. The major advantage of the method is that it does not impose any constraint on PSF extent, the information about the PSF size is difficult to obtain as required in

other algorithm.

The neural network approach of image restoration is emerging research area. The perception based adaptive approach of deconvolution by Stuart and Gaun is contribution to overcome spatial-variant type of degradation [19]. The concept of adaptive constraint parameter (ACP) restoration is introduced in order to cope with different statistical properties in different parts of an image.

## **1.6 Thesis Overview**

This thesis consists of 5 chapters. The first chapter provides an introduction about the problem and brief idea of different current approaches in the field of blind image restoration. Chapter 2 briefly describes about the commonly occurring blur. Chapter 3 presents the Evolutionary algorithm as a solution to gaussian blur. In Chapter 4 novel approach of motion blur estimation is presented. Chapter 6 concludes this thesis.

## **Chapter 2**

# **INTRODUCTION TO IMAGE BLUR**

The recognition and interpretation of actual information depends entirely on the image quality. Something that is hazy and indistinct to the sight that restrict the sound and clear visual perception have impact on image if captured at that instant. This ill-effect created from the indistinctness of information deteriorating the image quality while image acquisition is known as *blur*.

The basic approach for any deblurring technique is to acquire atleast minimal information about the blur caused. The various existing techniques to revert back the effect and reconstruct the true image depends on the quantitative yet effective knowledge about the cause of degradation. The fundamental method of image restoration is to estimate the parameters of degradation and then apply any classical restoration technique for image reconstruction[6]. The convergence of many *a priori* deconvolution techniques also demands for certain parameteric assumptions and estimation of image degradation[1]. The existing blind deconvolution techniques, such as IBD, [1] too rely on some initial estimation of the image[3].

## 2.1 The Point Spread Function,PSF

The degradation producing ill-effect of blur is termed as the *point spread function, psf*. Any type of blur is characterized by the *psf* . The electromagnetic radiation or other imaging waves propogated from a point source or point object is known as the *psf*. The quality of any imaging system depends on the degree of spreading(blurring) of the point object. The *psf* defines the impulse response of a point source[1]. This is shown in Figure 2.1. When an image is captured by any recording system, the intensity of a pixel of the recorded image is directly proportional to the intesity of the corresponding section of the sight be captured. But this is ideal situation. Practically, the recorded intensity either gets effected by the noise or blur.

### 2.1.1 Types of Blur

The *psf* causing degradation of any image are often two types as:

1. Spatial-variant blur
2. Spatial-invariant blur

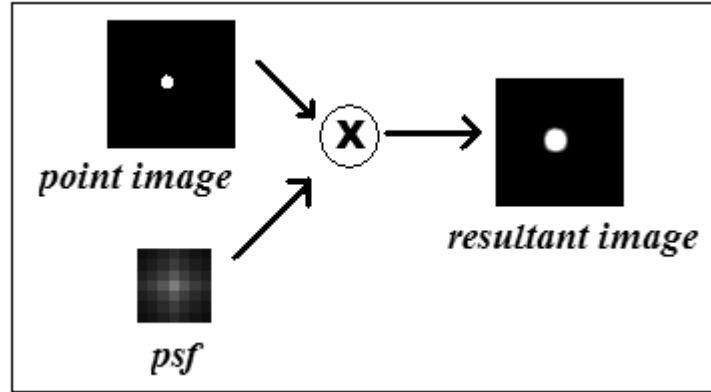


Figure 2.1: Image formation with PSF

The mathematical model for image formation can be reformulated by the linear equation[6]:

$$c = d_f i + \eta \quad (2.1)$$

where  $c$  is the observed blurred image,  $i$  is the true image  $\eta$  is the noise and  $d_f$  is the blurring function, the *psf*. The defocusing of any portion of the sight depends on the intensity and other characteristics of the corresponding section of the sight being captured. If the blurring is not distributed in a homogenous way, i.e, every pixel is defocused differently such that blur effects every pixel with varying strength, then the blur is known as *spatial-variant blur*. But if the image is blurred such that every spatial location is effected equally then it is considered as *spatial-invariant blur*. The degradation function, as stated in (1.1), is said to be *spatial-invariant* if for any shift  $k \in Z^2$ ,

$$c(x) = d_f[i(x)] \text{ implies that } c(x - k) = d_f[i(x - k)]$$

According to signal processing theory, this *shift-invariant linear function* is expressed in the form of *convolution*. So the above Equation 2.1.1, can be expressed in case of spatial-invariant blur as,

$$c(x, y) = i(x, y) * d(x, y) + \eta(x, y) \quad (2.2)$$

where  $'*$ ' indicates spatial convolution. The above eq, in discrete form is represented as,

$$c(x, y) = \sum_{m,n} i(m, n)d(x - m, y - n) \quad (2.3)$$

The above equation in an *frequency domain* can be written as :

$$C(u, v) = I(u, v)D(u, v) + N(u, v) \quad (2.4)$$

Thus blurring in this case is described as the convolution of the original image with a *psf*. Many restoration schemes assume that the *psf*,  $d$ , is spatially-invariant and spatial dependence is often ignored. But there are certain scenerios, where spatial variation of the degradation function has to be considered. For example, if the scene contains two objects moving with different velocities to the recording system, then the *psf* is effectively different for each [12]. Also in the case of original Hubble Space Telescope Wide-field/Planetary camera, due to errors in the shaping of the mirrors, the *psf* has a large amount of spatial variation[13].

The image restoration in space-invariant case is done by deconvolving the observed image with *psf*. In space-variant case, the *psf* at different regions are first estimated and the corresponding image region is deconvolved with it and finally, the different restored image regions are joined together to reconstruct the entire true image estimate. The process of modelling and image restoration in case of spatially-varying blur is more challenging problem as compare to spatially-invariant blur. The various types of *spatial-invariant blur* and their existing identification approaches has been described in the thesis.

## 2.2 Modeling space-invariant Blur

The difficulty in solving the restoration problem with a space-varying blur motivates the use of the stationary model of blur. The different models have been proposed in the literature for representing the space-invariant *psf*. The models can be described as:

1. Motion Blur: The moving objects when captured by the camera or the stationary object captured by moving camera cause motion blur. Many types of blur has been framed out in the literature. This can be in the form of a translation, a

rotation, a sudden change of scale or to some combination of these. But, here only the translation is considered. When the object is moving with a constant velocity  $V$  is being captured by the camera with an exposure time interval  $[0 T]$ , the distortion is given by[4]:

$$d(x, y; s, t) = \begin{cases} \frac{1}{VT} \delta(y - t), & 0 \leq (x - s) \leq VT \\ 0 & \text{otherwise.} \end{cases} \quad (2.5)$$

2. Out-of-focus Blur: When a sight is captured by the camera in a two-dimensional field, it may happen that some parts are in focus while other parts are not. The degree of defocus depends upon the effective lens diameter and the distance between the object and the camera[1]. This leads to the point-spread function:

$$d(x, y) = \begin{cases} \frac{1}{\pi r^2} & \text{if } (x^2 + y^2) \leq r^2 \\ 0 & \text{otherwise} \end{cases}$$

where  $r$  is the radius of the circle of confusion[4].

3. Atmospheric Turbulence Blur: The blur occurred due to the long-exposure through the atmosphere in certain application is modelled as the *gaussian psf*[3]. The psf in this case is given as:

$$d(x, y) = K \exp\left(-\frac{x^2 + y^2}{2\sigma^2}\right)$$

## 2.3 Motion Blur

When a photograph is taken of any moving object or the imaging system itself is moving then the degradation caused is *motion blur*. Motion blur causes significant degradation of the image. This is caused by the movement of the object relative to the sensor in the camera. The motion blur occurs if any of the following conditions persist,

1. Moving Object captured by static camera,
2. Static Object captured by camera in motion,
3. Both Object and camera are in motion,



4. Shutter movement, film is exposed in a camera by the movement of the shutter across the film plane.

The two types of motion blur has been studied. They are:

- Linear-Horizontal Motion Blur: The motion blur arising either to camera moving or the object moving horizontally is given as,  $L$  being the blur length. More precisely,  $L$  is the number of additional points in the image resulting from a single point in the original scene[4].

$$d(x) = \begin{cases} \frac{1}{L} & \text{if } \frac{-L}{2} \leq x \leq \frac{L}{2} \\ 0 & \text{otherwise} \end{cases}$$

- Angular Motion Blur: When the scene to be recorded translates at a constant velocity,  $V$ , with an angle of  $\theta$  degrees from the horizontal axis during the exposure interval,  $[0 T]$ , then the *psf* observed is given as[7]:

$$d(x, y) = \begin{cases} \frac{1}{L} & \text{if } 0 \leq |x| \leq L \cos \theta, y = L \sin \theta \\ 0 & \text{otherwise} \end{cases}$$

There are several techniques for prevention motion blur either during image capture or by using any *postprocessing* techniques to remove blur. The motion blur can be solved by adopting any of the following measure:-

- Using hardware in the optical system of the camera to stabilise the motion
- Post-processing technique by estimating the camera's motion from single image(blind deconvolution)

Hardware approach can be the solution but is effective for removing small amount of camera shake for short exposure. But this method does not involve any image processing method, so is not discussed. The motion deblurring as a post processing step can be done by estimating the motion blur parameters.

The post-processing techniques for motion blur estimation include Cepstral Analysis, Radon Transform, Steerable Filter [20]. Stern and Kopieka provided the analytical method of finding optical transfer function for image motion using moments [21]. A novel approach of identification of motion direction given only the blurred image is

presented by Tan and Zhang [22]. The thesis presents a heuristic approach of estimating the motion blur parameter. The algorithm exploits the fourier spectrum for direction estimation. This is discussed in detail in the chapter 4.

## 2.4 Gaussian Blur

The image degradation due to atmospheric condition is modelled by the gaussian effect. The gaussian blur is a type of image blurring filter that uses normal distribution for calculating the transformation to apply to each pixel in the image. The visual effect of this blurring is a smooth blur resembling that of viewing the image through the translucent screen.

The apparent "wobbling" distortion of scene when viewed through an open fire or across a hot road is well-known phenomenon. Similar effects is seen in the astronomical imaging also. These effects are due to gradient in the refractive index in the atmosphere resulting from temperature variation mostly. The visualization and characterization of the effect is of considerable interest to atmospheric scientists, earth-based astronomers and also for long-range surveillance. The deconvolution techniques are required for proper analysis in the scientific study. The research on various deblurring technique has been done in the literature to overcome this problem. The thesis presents the approach for restoring the image degraded due to gaussian effect by an Evolutionary algorithm. This is describe in detail in chapter 3.

## 2.5 Simulated Result

The standard lena image of  $256 \times 256$  is synthetically blurred with different types of blur. The blurred image are shown as in the figure 2.2. Figure 2.2(a) is Original Lena image, (b) Motion blurred image with  $L = 15$ ,  $\theta = 45^\circ$ , (c) Misfocussed image with  $r = 10$ , (d) Gaussian blurred image with  $\sigma = 0.85$ .



Figure 2.2: Result for different blur effect.

## **Chapter 3**

# **BLIND DECONVOLUTION USING EVOLUTIONARY ALGORITHM**

The recent development and the growing popularity of genetic algorithm in the various field, motivated the researchers to utilize the same in the field of image processing also. The evolutionary algorithm is the generic name for the genetic algorithm. The evolutionary algorithm (EA), in artificial intelligence, is a subset of evolutionary computation. It is generic population based metaheuristic optimization algorithm. An EA utilizes the concept of biological evolution. Evolutionary algorithms are search techniques based on the concept of natural selection and survival of the fittest in the natural world[8]. EA are computer programs used to solve complex problems by imitating the Darwins theory "survival of the fittest"[8]. In a EA a number of probable solutions are generated over the problem space. They then compete each other to find optimal area of the search space.

EA have number of operators, components and procedures that must be specified clearly in order to define particular EA[8]. Also, the initialisation and termination condition must also be well specified. The different components of EA are:-

- Definition of Individuals
- Fitness Function
- Population
- Recombination Mutation
- Survivor Selection Mechanism

Unlike other traditional optimization techniques, EA involve a search from set of possible solutions known as "population". Each iteration ends with a set of possible and feasible solutions, discarding the poor solutions based on some "fitness" criteria. The solutions with high fitness are then recombined with other solutions by interchanging parts of the solution with one another. These solutions are then again "mutated" generating new solution optimal to the given problem. The scheme is shown in Figure 3.1. Several types of evolutionary algorithm search techniques were developed independently. The history of the technique suggests that there are number of variants of the EA, but the basic underlying idea is same:-from the given population, only the fittest candidates are opted for the solution space. Some of the flavors of EA are:-

- Genetic Programming, which evolve programs

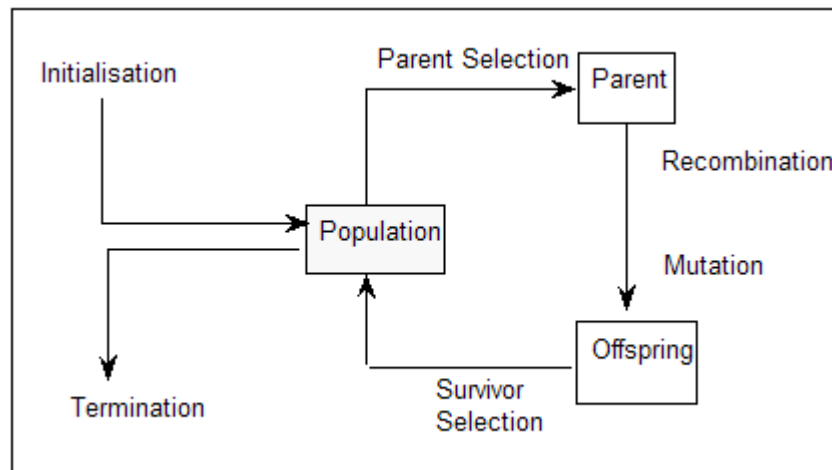


Figure 3.1: General scheme of EA

- Evolutionary Programming, which focusses on optimizing continuous functions without recombinations
- Evolutionary Strategies, which focusses on optimizing continuous functions with recombinations
- Genetic Algorithm, which focuses on optimizing general combinatorial problem.

### 3.1 Applications of Evolutionary Algorithm, EA

Evolutionary algorithm is considered as global optimization technique. The most important factor about EA is its robust performance in "noisy" functions where there is multiple local optima. EA can find global optimal solutions discarding the local minima. There exists wide variety of application domains of EA for finding optimization problems such as wire routing, scheduling, travelling salesperson, image processing, engineering design, parameter fitting, knapsack problem, game playing and transportation problem. EA are well suited for wide range of combinatorial and continuous problems [8], but the different variations are tailored depending upon specific applications. The concept of EA has been utilized in the field of image processing. Different image processing area such as edge detection, segmentation, shape detection, feature selection, clustering, classification, object recognition use EA to get the optimal

solution.

## 3.2 Multiobjective Optimization using EA

The purpose of simulating the evolutionary process, following the analogy between evolutionary mechanism and the learning process (optimization), led to the development of evolutionary algorithm. Multi-objective optimization is the fastest growing technique in the recent years among many other emerging techniques of EA. In multiobjective problem, there is no single objective and possibly no single solution. The solution is selected from a set by making compromises. A suitable solution is chosen satisfying the different objectives.

The main motivation for using EA for solving multi-objective optimization problems is because EAs deal simultaneously with a set of possible solutions (the so-called population) which allows us to find several members of the Pareto optimal set in a single run of the algorithm [8], instead of having to perform a series of separate runs as in the case of the traditional problem solving approach.

## 3.3 EA for Blind Deconvolution

The development and successful application of EA in different complex problem motivates to utilize the concept in the field of blind image deconvolution. The blind deconvolution is the practical method of image reconstruction, when it is not possible to reconstruct the image with all *psf*. The EA provides large solution space for the deconvolution and then the optimized solution is selected.

## 3.4 Underlying Assumptions

The image model as in Equation 1.3 is considered. So, an ideal noiseless scenario is assumed. As a matter of convenience, the model is again re-written below:-

$$c(x, y) = i(x, y) * d(x, y) \quad (3.1)$$

The algorithm proceeds based on following main identity:-

$$i(x, y) = i(x, y) * \delta(x, y), \quad (3.2)$$

where  $\delta$  is finite with all its elements zero except the central one ,given as,

$$\delta = \begin{pmatrix} \dots & \dots & \dots & \dots & \dots \\ \dots & 0 & 0 & 0 & \dots \\ \dots & 0 & 1 & 0 & \dots \\ \dots & 0 & 0 & 0 & \dots \\ \dots & \dots & \dots & \dots & \dots \end{pmatrix}$$

where  $\delta$  is finite square matrix with all its element zero but the central element is one. The *psf* is supposed to composed of two matrices given as,

$$d_L(x, y) + d_H(x, y) = \delta(x, y) \quad (3.3)$$

where  $L$  and  $H$  denotes for low and high, respectively. Hence,( 3.2) can be rewritten as,

$$i(x, y) = i(x, y) * d_L(x, y) + i(x, y) * d_H(x, y) \quad (3.4)$$

Now, if the observed blurred image,  $c$ , in(3.1) is given by

$$c(x, y) = i(x, y) * d_L(x, y) \quad (3.5)$$

then an iterative approach is derived based upon the following two equations:

$$\hat{i}(x, y) = c(x, y) + \tilde{i}(x, y) * \hat{d}_H(x, y) \quad (3.6)$$

$$\hat{c}(x, y) = \hat{i}(x, y) * \hat{d}_L(x, y) \quad (3.7)$$

where  $\tilde{i}(x, y)$  and  $\hat{i}(x, y)$  denote the consecutive iterative estimations of the true image  $i(x, y)$  at generation  $k$  and  $k+1$ , respectively. At every iteration, the *psf*,  $\hat{d}_L(x, y)$  is randomly generated and  $\hat{d}_H(x, y)$  is obtained by using(3.3).



### 3.5 Underlying Constraint on PSF and Image

The blind deconvolution using EA assume some constraint on the PSF and the Image. The PSF constraint assume that the blur function should be positive and the mean value of the image is preserved during degradation. That is,

$$\sum_{(x,y) \in S} \hat{d}_L(x, y) = 1 \quad (3.8)$$

where  $S$  is the finite support of the textitpsf,  $\hat{d}_L(x, y)$ . Also, the blurring function should be symmetric with zero-phase[8]. Similarly, the algorithm assumes that the pixel value restored image should be positive. And, the pixel intensity strictly lies between 0 and 255, considering only gray scale image. The image constraint can be formulated as,

$$\begin{aligned} \text{if } \hat{i}(x, y) \leq 0 \\ \hat{i}(x, y) &= 0 \\ \text{if } \hat{i}(x, y) \geq 255 \\ \hat{i}(x, y) &= 255 \end{aligned}$$

### 3.6 Convergence Criteria

In order to control the convergence of the algorithm, the two feature vectors are used, denoted as  $\rho_1$  and  $\rho_2$ [8]. The  $\rho_1$  is a peak signal-to-noise ratio between  $c$  and  $\hat{c}$ . The optimal estimate of  $i(x, y)$  is the one that corresponds to the output  $\hat{i}(x, y)$  with the highest  $\rho_1$  value. Similarly, the  $\rho_2$  is defined as a peak signal-to-ratio between  $\hat{i}(x, y)$  and  $c$ . The optimal estimate of  $i(x, y)$  corresponds to the output  $\hat{i}(x, y)$  with a  $\rho_2$  value closest to a given minimum. The two conditions are used as a convergence criteria of the algorithm, collectively denoted as,  $\rho = (\rho_1, \rho_2)$ , called as feature vectors[8].

### 3.7 Realizing BID using EA

The EA for BID can be implemented using by incorporating different steps EA with the deconvolution steps. The EA provides large solution space thus easying to get optimal

Table 3.1: Algorithm for PSF generation

1.	Find the <i>psf</i> size, $n \times n$ , $n$ should be odd number.
2.	Randomly generate $\frac{n+1}{2}$ values in the range (0, 1).
3.	Sort the values generated in ascending order.
4.	Produce a vector $d_1$ of $n$ elements, by flipping the values left to right provided the middle element is untouched.
5.	Create $d = d_1 * d_1^T$ .
6.	Finally, normalize the $d$ .

solution. The basic steps adopted for achieving the objective is shown in the schematic Figure 3.2. The major steps followed are:-

- **Mutation:-** A set of random *PSFs* is generated in every generation. These *PSFs* are then used along with all individual images, obtained from the previous generation. This is done by following Eq. 3.6 and (3.7).
- **Selection:-** The individuals in each generation individually undergo a selection procedure, as stated previously, called feature vectors. Those individuals which have  $\rho_2$  value greater than the corresponding expectation value for the generation are excluded.
- **Clustering:-** There exist only few individuals at each generation. The survivors are used in the next  $k + 1^{th}$  generation. The stopping criterion,  $|\hat{\rho}_2^k - \rho_2| \leq \varepsilon$ , is checked at each iteration. And  $\hat{\rho}_2^k$  is the average estimated value of  $\rho$  at  $k^{th}$  generation and  $\varepsilon$  should be greater than 0 and is experimentally determine.
- **Final Image Reconstruction:-** There is set of possible estimated image obtained from each generation at the end. The best image is sort out by adopting fusion method, *pseudowigner distribution, pwd*. The detail about *pwd* is discussed in the next section.

The steps for generating set of *psf* generated in every generation is shown in the Table 3.1.

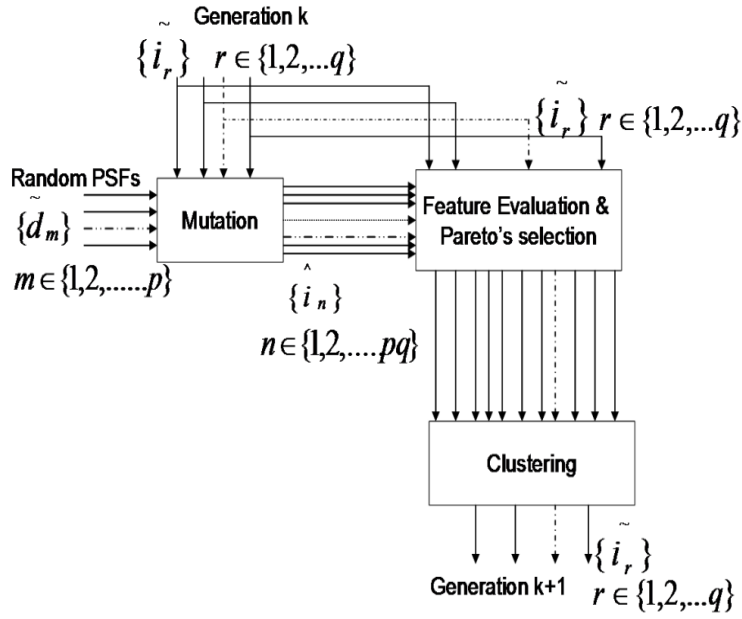


Figure 3.2: General scheme of BID using EA

### 3.8 Image fusion using *pseudo-wigner distribution, PWD*

The fusion method used is based on the existence of inut realization of different input realizations of the same object at the same time. The distance between the *pseudo-wigner distribution, pwd* of the images to the *pwd* of the reference image  $\mathcal{c}$ , on a pixel by pixel is computed to perform deblurring. The Wigner distribution of 1-D function  $s(x)$  is given by[9]:-

$$W(x, u) = \int_{-\infty}^{\infty} s(x + \frac{\alpha}{2})s^*(x - \frac{\alpha}{2}) \exp^{-i(u*\alpha)} d\alpha \quad (3.9)$$

In this algorithm, a discrete Wigner distribution is used, formulated as below,

$$W(n, m) = 2 \sum_{k=-\frac{N}{2}}^{\frac{N}{2}} s(n+k)s^*(n-k) \exp^{-2i(2\pi\frac{m}{N})k} \quad (3.10)$$

where,  $n$  and,  $m$  represent the spatial and space-frequency respectively, and  $k$  is the shifting parameter. Equation(3.10) is interpreted as the discrete Fourier transform (DFT) of product  $r(n, k) = s(n+k)s^*(n-k)$ . Different  $N$ -component PWD vector associated with every pixel on the image is computed and the measure is adopted for determining their greatest distance to a reference image. The more defocused an im-

age is the more the high frequencies get diminish and hence, its *pwd* is affected. The observed blurred image is taken as refernce. This helps in establishing at pixel level a distance measurement for the *PWD* from each image,

$$\Delta_i(\xi) = \|W_i(n, m) - W_r(n, m)\|_{n=\xi} \quad (3.11)$$

where  $\xi$  denotes an arbitrary pixel of the image,subindices  $i$  and  $r$  indicates input and reference images, respectivel.  $W_i(n, m)$  represents the *PWD* for the reference image. The norm operator in (3.11) is given as:-

$$\|\xi\| = \left( \sum_{i=-\frac{N}{2}}^{\frac{N}{2}} \xi^2(i) \right)^{\frac{1}{2}} \quad (3.12)$$

where  $\xi$  represents any arbitrary real vector. The largest Euclidean distance corresponds to the pixel belonging to the less locally defocused image[8]. All pixels from the  $p$  input images can be ordered following the same.

### 3.9 Simulation Results of EA

The algorithm is worked out to reconstruct the image degraded due to atmospheric turbulence, commonly modelled as the gaussian psf. Three images have been used for the simulation purpose, the standard lena image of size  $64 \times 64, 128 \times 128$  and the lake image of size  $128 \times 128$ . The gaussian psf of size  $7 \times 7$  with  $\sigma = 0.65$  and  $\sigma = 0.85$  is convolved with lena image of size  $64 \times 64$  to artificially generate atmospheric turbulence degraded image. Similarly, lena image of size  $128 \times 128$  is synthetically blurred using psf of size  $15 \times 15$  and the  $\sigma = 0.85$ . The lake image is also artificially blurred using varying psf size with  $\sigma$  values being 0.34,0.65 and 0.85 respectively. The synthetically generated blurred figures and the corresponding restored are shown in Figures. Figure 3.3(a) shows Lena image blurred with  $\sigma = 0.65$ , (b) is restored image. Figure 3.4(a) depicts Lena image blurred with  $\sigma = 0.85$ , (b) is corresponding restored Image.Similarly, Figure3.5(a) shows Lena image blurred with  $\sigma = 0.85$ and (b) is restored image. Figure 3.6 shows blurred Lake Image, (a) is blurred with  $\sigma = 0.34$  and (b) is restored image,(c) shows image blurred with  $\sigma = 0.55$  and (d) is restored image of (c),(e) depicts image blurred with  $\sigma = 0.85$  and (f) is corresponding restored

image.



Figure 3.3: Gaussian Blurred Lena Image and Restored Lena Image



Figure 3.4: More Gaussian Blurred Image Lena Image and Restored Image



Figure 3.5: Gaussian effected Lena Image

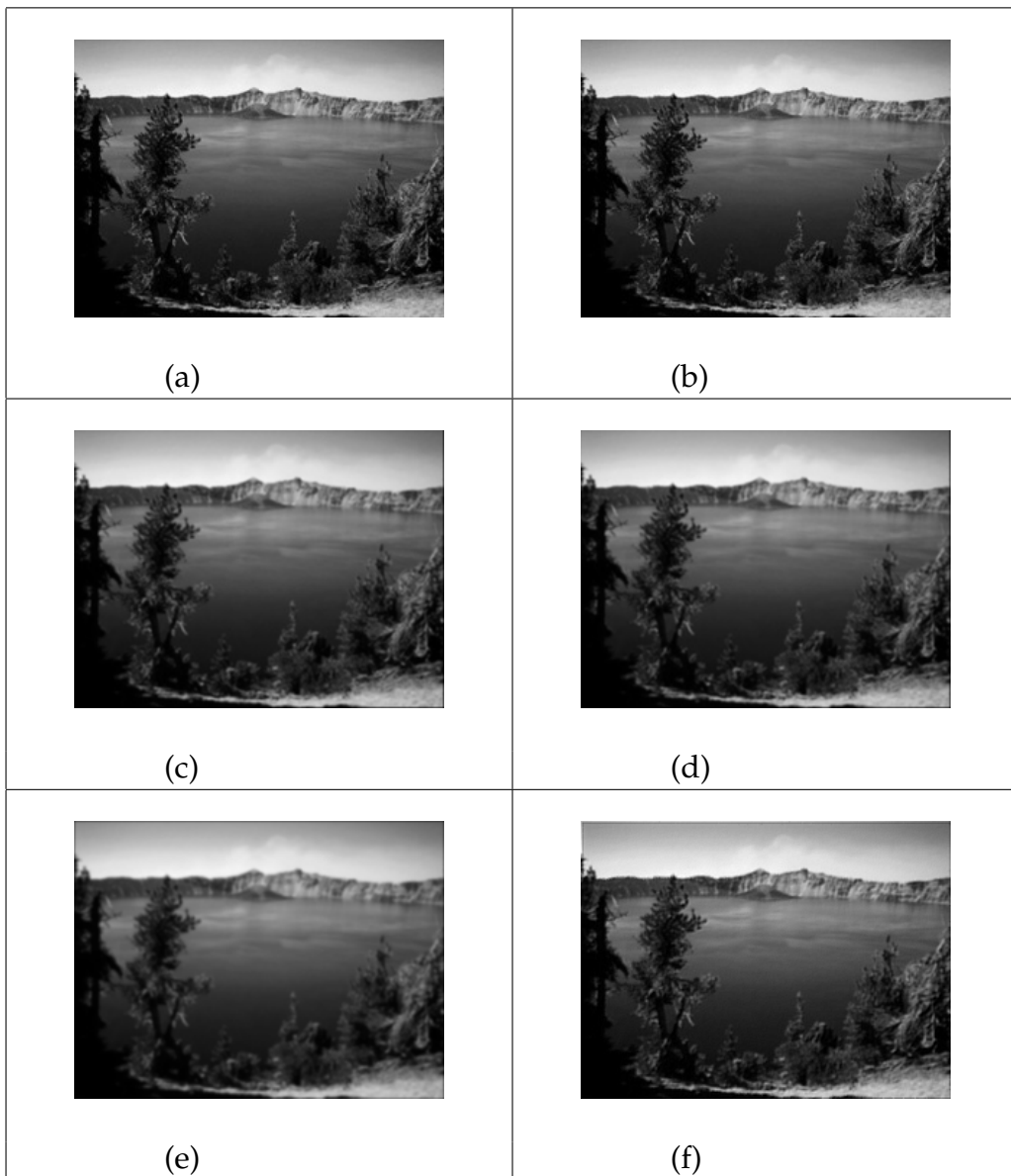


Figure 3.6: Gaussian blurred lake image with varying value of standard deviation.

## **Chapter 4**

# **TWO PASS HEURISTIC APPROACH FOR MOTION BLUR PARAMETER IDENTIFICATION**

*Deconvolution* is an engineering discipline, which refers to the retrospective improvement of fidelity of the electronic signals such as voice, music, radar and pictures. Image processing utilizes the same concept in restoring the true image from degraded image. The input is the corrupted natural image and one of the many existing deconvolution techniques is used to retrieve the true image. But this restored image is the estimation of the true image and hence the convergence of deconvolution techniques should provide the approximate and closest estimate of the true image. The blind image deconvolution on similar concept estimate the true image but there are almost no or partial information about the cause of degradation function. The partial information can be in the form of some finite support or nonnegativity of the image, coined as physical properties of the image. Similarly, this partial information can also be in the form of any statistical data such as entropy or probability distribution function of the signal. The different optimality criteria along with this partial information form the strong ground in image estimation.

The Visual world around us is always dynamic. The moving objects when captured with any imaging system leads to ill-effect known as *motion blur*. The degraded image can be restored if the motion blur parameters can be identified. Once the blur has been estimated, the classical restoration can be utilized to restore the degraded image. This blind technique of restoring the degraded image by first computing the *psf* and then utilizing any of the classical restoration technique comes under *a priori technique*.

## 4.1 Motivation for Blur Identification

Blind deconvolution techniques have always been a challenging and critical problem. But, since the techniques are more useful for the practical scenerio compared to classical ones, the methods can not be ignored. Different blind image deconvolution techniques assume various parameter to solve the problem. The literature review on different techniques reveal that some strong underlying concept has to be used as a key to crack the problem. Though the convergence is not well-defined as well as not sure. This motivates to search for the parameters responsible for degradation. The parameter once estimated is used to reverse the *ill-effect*. This chapter is contribution towards motion blur identification.

The motion blur is caused whenever there is relative motion between the object



and the imaging system. This blur can be estimated if the *length* of the blur and the *direction* can be somehow computed.

## 4.2 Theoretical Background

The 2-D *discrete fourier transform*, (DFT) of any  $f_1$  representing any MxN image, denoted by  $F(u, v)$ , is given by the equation[6] ,

$$F_1(u, v) = \sum_{x=0}^{M-1} \sum_{y=0}^{N-1} f(x, y) \exp^{-j2\pi(\frac{ux}{M} + \frac{vy}{N})} \quad (4.1)$$

for  $u = 0, 1, 2, \dots, M - 1$  and  $v = 0, 1, 2, \dots, N - 1$ . The *exponential* could be expanded into sines and cosines with the variables  $v$  and  $u$  determining their frequencies. Since  $f_1$  being an image so it is real, but its *fourier transform* in general is complex. The principal method of visually analyzing the transform is to compute its spectrum[i.e.,the magnitude of  $F_1(u, v)$ ] and display it as an image. Let  $R_l(u, v)$  and  $I_m(u, v)$  represent the real and imaginary component of  $F_1(u, v)$ , the *fourier spectrum* is defined as,

$$|F_1(u, v)| = [R_l^2(u, v) + I_m^2(u, v)]^{\frac{1}{2}} \quad (4.2)$$

The phase angle of the transform is defined as,

$$\phi(u, v) = \tan^{-1} \left[ \frac{I_m(u, v)}{R_l(u, v)} \right] \quad (4.3)$$

The above two equation can be used to represent  $F_1(u, v)$  as below,

$$F_1(u, v) = |F_1(u, v)| \exp^{-j\phi(u, v)} \quad (4.4)$$

The observed degraded image is nothing but the convolution of the true image with some degradation function. This is true in the spatial domain. In the *frequency domain*, the convolution is multiplication of the corresponding fourier transform of the functions.

$$C(u, v) = I(u, v)D(u, v) \quad (4.5)$$

Substituting the value of  $I(u, v)$  and  $D(u, v)$  by following the definition of *fourier* derived

in the(4.4) in (4.5), we get,

$$C(u, v) = |I(u, v)| \exp^{-j\phi_i(u,v)} |D(u, v)| \exp^{-j\phi_d(u,v)} \quad (4.6)$$

Similarly subsequently substituting for  $C(u, v)$  in above equation. 4.6, the same *fourier* definition,the resulting equation is,

$$|C(u, v)| \exp^{j\phi_c} = |I(u, v)| \exp^{-j\phi_i(u,v)} |D(u, v)| \exp^{-j\phi_d(u,v)} \quad (4.7)$$

Equating the exponential parts of both the sides, omitting  $u$  and  $v$  for convinience, we have,

$$\phi_c = \phi_i + \phi_d \quad (4.8)$$

Thus the phase of the observed image is the addition of the phases of the true image and the degradation function both. Figure4.1 depicts the fourier spectrum plotted for lena image blurred with angle  $\in 0^0, 15^0, 30^0, 45^0$  respectively.

The degradation process can thus be understood as a filtering in the spatial domain consisting of the true image  $i(x, y)$  with a filter mask,  $d(x, y)$ . According to the convolution theorem, we can obtain the same result in the frequency domain by multiplying  $I(u, v)$ , the *fourier transform* of the true image by  $D(u, v)$ , the *fourier transform* of the filter. The  $D(u, v)$  is commonly referred as the *filter transfer function*. This  $D(u, v)$  is the function that modifies  $F(u, v)$  in a specified manner. Hence, when formulated as motion blur function, the filter operates on the *frequency spectrum* of the true image inturn. The motion blur used is linear shift-invariant in nature and is characterized by the length of the blur and the angle. Thus, when the filter operates on the true image, the angular information of the mask gets embedded in the image along with other parameters. This can be easily visualize in the *fourier spectrum* of the degraded image.

The angular information is investigated and the length is then computed by estimating the approximate of the true image. The quality of the estimated image is measured using the *Shannon Entropy*. It is well-known that the digital image is a realization from a source  $S$  generating symbol,  $s_i$ , identified as the gray values of the image. Associated with a symbol source  $S$ , there is a number,  $H(S)$ , called the *entropy* of the source, which measure the amount of information in the source. The *entropy* of a source  $S$  is defined

by,

$$H(S) = - \sum_{i=1}^q P(s_i) \log_2 P(s_i) \quad (4.9)$$

where  $P(s_i)$  = number of times  $s_i$  occurs in the image  $M \times N$ .  $M \times N$  is the size of the image and  $q$  the number of gray levels in the source, i.e., 256 for a 8bits/pixel image. The estimated image with the values closer to the highest *entropy values* are again checked using othe metric , *RMSE*, with reference to the observed blurred image. The *RMSE* between two images say,  $F_1$  and  $F_2$  is given as,

$$RMSE(F_1, F_2) = \sqrt{\frac{\sum_{x=1}^N \sum_{y=1}^M [F_1(x, y) - F_2(x, y)]^2}{N * M}} \quad (4.10)$$

### 4.3 Implementing the Algorithm

The approach adopted here starts with closely visualizing the Fourier spectrum of the blurred image. Whenever the image suffers from motion blur, the direction of the motion is well preserved in the *fourier* domain of the blurred image. This can be clearly analyze from the figure.4.1.

The angular direction gets captured in the fourier spectrum. The periodic black-white band subtend the angle with the verical axis from the origin. Thus, the fourier spectrum of the blurred image is utilized to get an approximate value of the motion direction. This angle is roughly computed to get an closer value of the actual blur angle.

The bright band passing through the origin is used to get a close approximation of the angular direction. A pixel with a maximum intensity can be traced out at some radial distance from the origin. The radial distance is set and the pixel is searched for each degree of rotation. Here, the search has been done for the angles ranging from 0 to 90 degree. The angle which gives the maximum intensity pixel at radial axis being set before is the required rough estimated direction. The approximate angle so obtained is then ranged to get the more refined angle. For each value of the angle in the newly approximated domain, the length is estimated. For each value of length the *psf* is computed and the image estimate is obtained. The image estimate is then used to calculate the *entropy* of the corresponding image. The image estimates with the entropy values closer to the highest entropy of the all estimated image are sorted out. These

image estimate are further tested for closed approximation of the true image. This is done by computing the *RMSE, root mean square error* with referenced to the observed image. This steps helps in filtering out the image estimates that have entropy closer to the high value but contains no information.

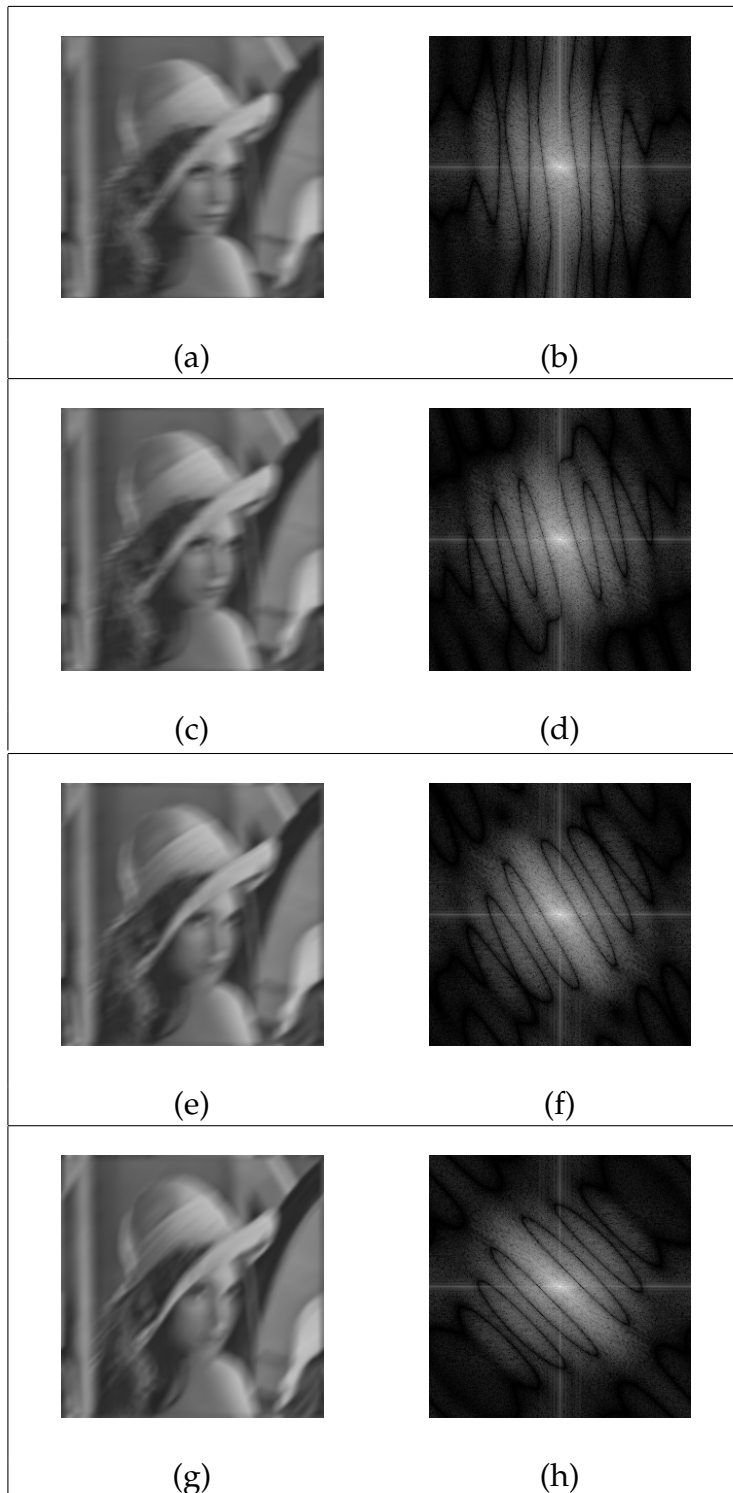


Figure 4.1: Motion Blurred Lena Image with varying angle and its corresponding Fourier Spectrum

The computed *RMSE* values are then arranged in the ascending order. The length and the angle corresponding to the minimum *RMSE* is the required parameter. The different algorithm steps are tabulated as below:

Table 4.1: Algorithm

- 
- 
1. Find *FFT* of the given blurred image  $c$ ,  
 $C1 = \mathcal{F}(c)$ .
  2. Shift  $C1$  to origin.
  3.  $C2 = \log(1 + |C1|)$
  4. Find the approximate angle subtended by the spectrum  $C2$  to the origin from vertical axis,  $A_{init}$ .
  5. Variate the approximated angle from  $-\alpha$  to  $\alpha$ ,  $A = \{-\alpha + A_{init} : \alpha + A_{init}\}$ .
  6. For each value of  $A$  and length,  $L = \{3 : \frac{\text{sizeof}(c)}{2}\}$ , calculate the *psf*. Obtain Image estimate for each *psf*.
  7. Compute Entropy for each estimated image.
  8. Obtain angle and length of the estimated image giving values closer to the maximum entropy.
  9. Calculate *RMSE* using the filtered image at step8 with respect to blurred image.
  10. The parameters giving minimum *RMSE* is the required angle and length.
- 

## 4.4 Simulation Result

The proposed algorithm is simulated for standard grayscale Lena image of size  $64 \times 64$ . The true ground image is synthetically blurred with the *psf* of varying length and angle. The *psf* length is varied from 5 to 30. The motion blur with angle ranging from  $0^0$  to  $45^0$ . The approximated angle range is increased using  $\alpha = 5$ . The entropy is iteratively caluted by using the estimated angle but with varying blur length. This provide with a solution space consisting of high entropy value. But, the true image estimate entropy lies closer to the highest entropy among all. This can be observed from the Figure 4.3.

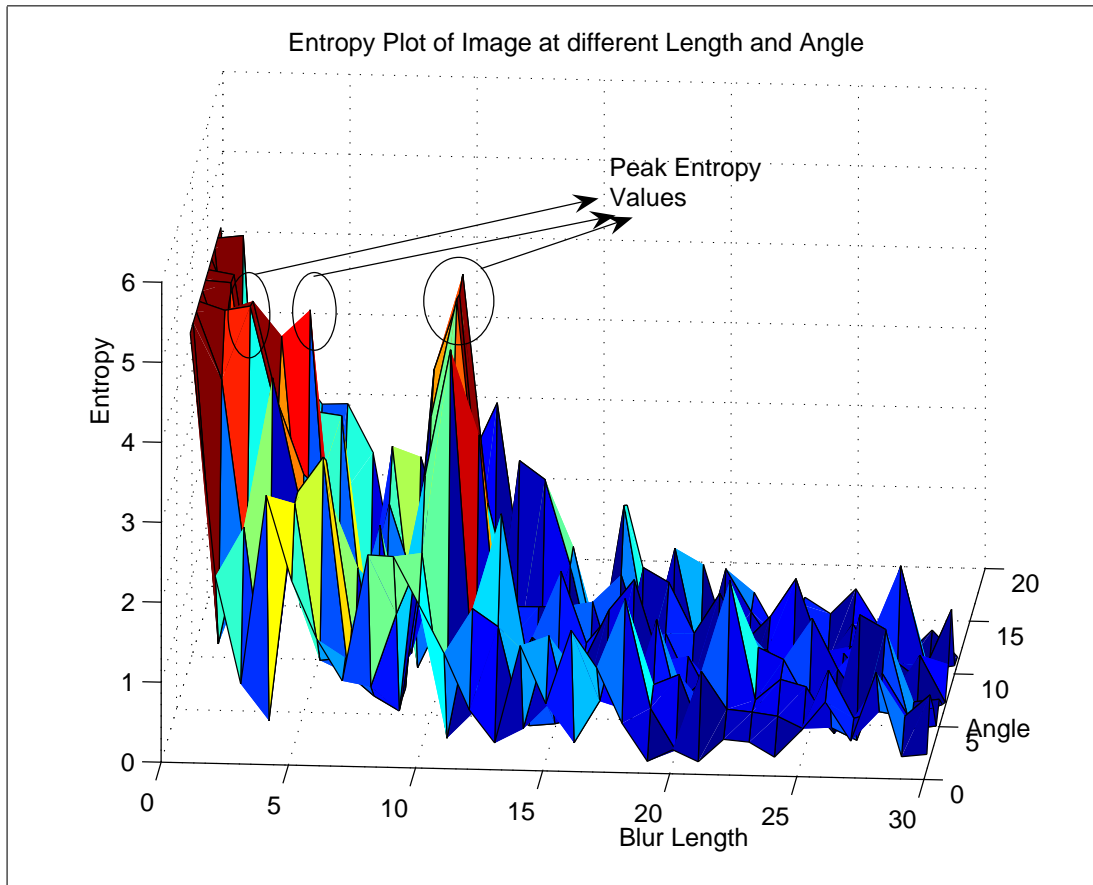


Figure 4.2: Plotted Entropy of images.

Figure 4.2 depicts the entropy plot of the images estimated for blurred image with Length=11 and  $\theta = 15^\circ$  which shows prominent peaks at various places. Similarly, Figure 4.3 is entropy plot of the images estimated for image blurred with Length=17 and  $\theta = 17^\circ$  which shows peak at different places including at desired place. The prominent peaks at some value of angle and length actually correspond to informative image estimate but not exactly the true image. Some of these estimate correspond to the obsolete result. To get rid of these estimates, the estimated image are again chosen based on the *RMSE* with reference to the observed blurred image. Then the minimum *RMSE* correspond to the desired length and the angle. The image is then restored using the classical inverse filter. The following figure shows the restoration. The  $64 \times 64$  lena image is blurred with the *psf* of length=11 and  $\theta = 23^\circ$ . The result is shown in the figure 4.4. The ground image is blurred with different values of the *psf*. The algorithm shows the good result till length=25. The result is tabulated in the Table 4.4, showing succesful estimation in many cases tested. The deviations are obtained mostly when the image is blurred with length greater than half of its size. But the result includes

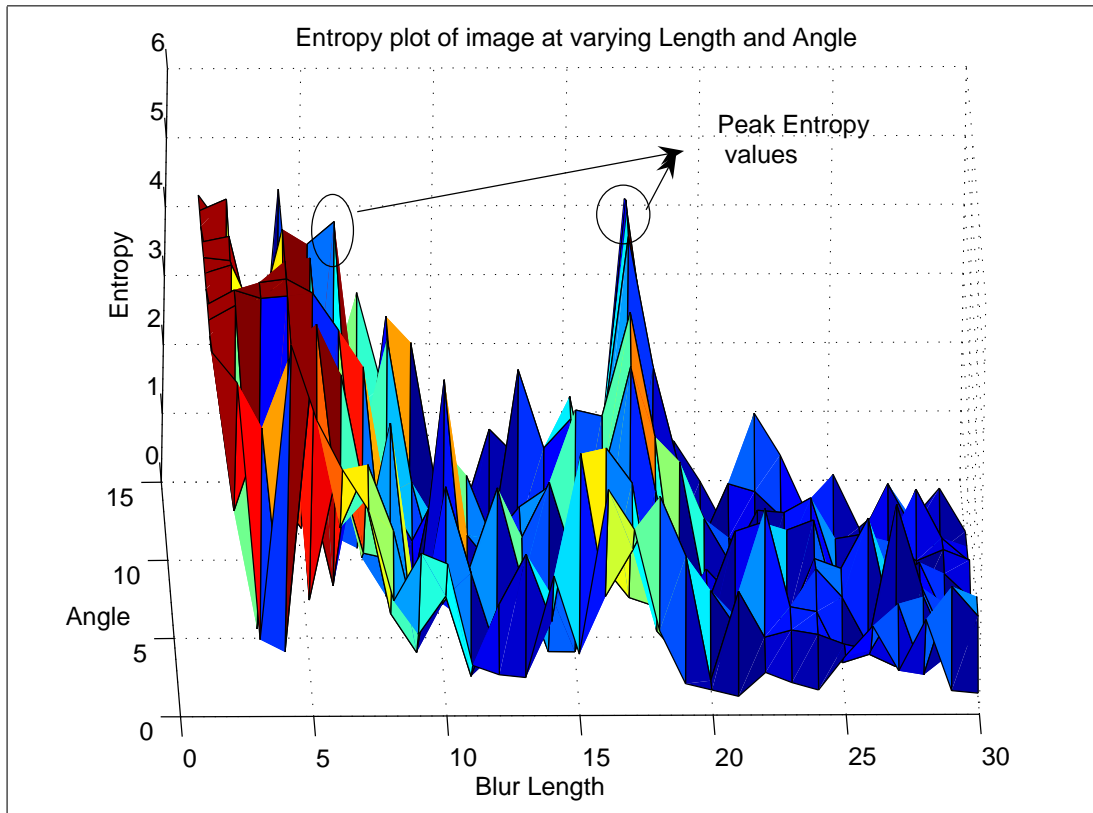


Figure 4.3: Entropy plot of images.

more number of favourable solution as compare to the obsolete ones.

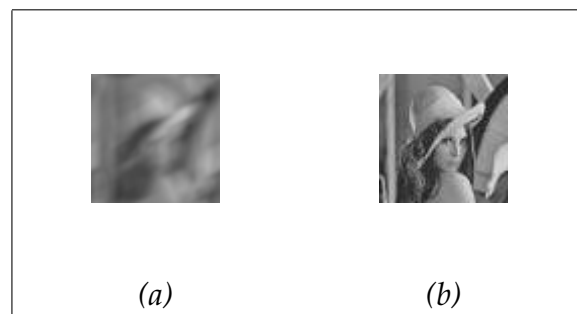


Figure 4.4: (a) Lena image blurred with psf length=11 and angle=23. (b) Restored image.



Table 4.2: Results of Observed Blur Parameter

Actual	Observed
Length & Angle	Length & Angle
7,0	7,0
7,45	7,45
11,45	11,45
13,19	13,20
15,25	15,25
9,19	9,19
7,30	7,32
15,19	15,19
23,45	23,45
7,19	7,24
27,23	27,23

## Chapter 5

# CONCLUSIONS AND FUTURE WORKS

Optically stabilised lenses are often used in video cameras and more expensive still cameras to reduce the effects of small amounts of camera shake. These use a system of gyroscopes and inertial sensors to keep the optical systems of the camera steady during image capture. This is only really effective for removing a small amount of camera shake at relatively short exposures (less than 1/15th second). Due to this hardware incapability, the image blurring is unavoidable in practical scenarios, and the required information is lost. Human visual system is primary tool for the information extraction from the blurred image. But this is possible only if the information is lost up to certain extent due to blurring. Hence, the image deblurring techniques has to be applied.

For practical applications, the exact modelling of the system is always not possible, thus, we go for blind technique for image deblurring. The focus in this thesis is the motion blur and the gaussian blur. To overcome the gaussian blur, the evolutionary algorithm is used. Even for maximum standard deviation, this simulation shows satisfactory result. A novel heuristic approach is introduced to estimate motion blur parameters. This algorithm is tested for varying motion direction and blur length.

The field of blind image deconvolution is critical as well as challenging problem. The thesis has been worked out considering only spatial-invariant type of blur to reduce the problem complexity. But spatial-invariant blur fails to model the blur in most of the practical case[24]. The noise effect is considered zero which is normally impractical. The irreducible demand of psf for unambiguous deconvolution is another limitation. The ground truth image used is grayscale and is synthetically blurred. The

blind image deconvolution approach adopted requires a well classification of the type of the degradation that the image has undergone, and then a particular method could be applied.

The thesis can be more useful for practical application if the spatial-variant degradation and noise parameters are considered. This opens the future research of the current work leading to robustness of the algorithms. The work can also be extended for the color images.

# Bibliography

- [1] Kundur Deepa,Hatzinakos,"Blind Image Deconvolution", *IEEE Signal processing Magazine*, 13(6) May(1996), pp.43-64.
- [2] Kundur Deepa,Hatzinakos,"Blind Image Deconvolution Revisited", *IEEE Signal processing Magazine*, 13(6) November(1996), pp.61-63.
- [3] Jiang Ming,Wang Ge,"Development of blind image deconvolution and its application", *Journal of X-Ray Science and Technology*,IOS Press,11(2003),pp. 13-19.
- [4] Biemond Jan, L.Lagendijk Reginald, M. Mersereau Russell ," Iterative Methods for Image Deblurring", *Proceedings of the IEEE*, vol 78,No.5, May 1990, pp.856-883.
- [5] Jain Anil K.,"Fundamentals of Digital Image Processing", Davis:Prentice-Hall of India, 2000.
- [6] Gonzalez C.Rafeal, Woods Richard E., "Digital Image Processing", London:Pearson Education, 2002.
- [7] Lokhande R., Arya K.V., Gupta P., "Identification of Parameters and Restoration of Motion Blurred Images", *SAC'06, France*, April 23-27 2006, pp.301-305.
- [8] Gabarda Salvador, Cristobal Gabriel, "An evolutionary blind image deconvolution algorithm through the pseudo-Wigner distribution", *Science Direct, J. Vis. Commun. Image R.*, July 2005, pp.10401052.
- [9] Dragoman Daniela, "Applications of the Wigner Distribution Function in Signal Processing", *EURASIP Journal on Applied Signal Processing*, vol 10, 2005, pp.15201534.
- [10] Gabarda S., Cristobal G., " Multifocus image fusion through the pseudo-Wigner distribution", *Opt. Eng.*, vol. 44 (4), (2005), 047001-1/047001-9 .

- [11] Kostas T.J., Mugnier L., Katsaggelos A.K., and Sahakian A.V., A Super-Exponential Method for Blur Identification and Image Restoration, SPIE Conf Visual Commun. and Image Processing, October 1994, pp.921-929.
- [12] Savakis A.E., Trussell H.J., "Blur identification by residual spectral matching", *IEEE Trans, Image Processing*, Feb 1993, pp.141-151.
- [13] Biretta J., " WFPC and WFPC2 Instrumental Characteristics, in the Restoration of HST images and Spectra-2", Space Telescope Science Institute, Baltimore, MD, 1994, pp.224-235.
- [14] Lane R. G., Bates R. H. T., Automatic multidimensional deconvolution, *J Opt Soc Am A*, vol. 4(1), January 1987, pp. 180-188.
- [15] Cannon M., "Blind deconvolution of spatially invariant image blurs with phase", *IEEE Trans Acoust, Speech, Signal Processing*, vol.24(1), February 1976, pp.58-63.
- [16] Chalmond B., "PSF estimation for image deblurring", *CVGIP: Graphical Models and Image Processing*, vol.53(4), July 1991, pp.364-372.
- [17] Chang M.M., Tekalp A.M., and Erdem A.T., "Blur identification using the bispectrum," *IEEE Trans Signal Processing*, vol.39(10), October 1991, pp.2323-2325.
- [18] Ayers G.R., Dainty J.C., "Iterative Blind Deconvolution method and its application", *Optics Letter*, vol.13(7), July 1988, pp.547-549.
- [19] Perry, Stuart W., Guan Ling, Perception Based Adaptive Image Restoration, *Proc. IEEE International Conference on Acoustics, Speech and Signal Processing*, Seattle, Washington, USA, vol.5, May(12-15) 1998 pp. 2893-2896.
- [20] Kraemer Felix, Lin Youzuo, McAdoo Bonnie, Ott Katharine, Wang David, Widemann Jiakou, "BLIND IMAGE DECONVOLUTION: MOTION BLUR ESTIMATION", Aug 18(2006).
- [21] Stern A., Kopeika N.S., "Analytical method to calculate optical transfer functions for image motions and vibrations using moments", *Optical Society of America*, vol 14(2), February 1997, pp.388-396.

- [22] Tan Wenzhao, Zhang Jin, Rong Gang, Chen Huirng, "Identification of Motion Blur Direction Based on Analysis of Intentional Restoration Errors", Proceedings of 2004 IEEE, March 21-23(2004), pp 1253-1258.
- [23] Mou-yan Zou and Unbehauen R., "A few new algorithms of 2-D blind deconvolution", Optical Engineering, vol.34, no. 10, 1995, pp. 2945-2956.
- [24] Nagy James G., O'Leary Dianne P., "RESTORING IMAGES DEGRADED BY SPATIALLY VARIANT BLUR", SIAM J. SCI. COMPUT., vol. 19, no. 4, July 1998, pp. 1063-1082.